

Received March 31, 2019, accepted April 18, 2019, date of publication April 26, 2019, date of current version May 7, 2019.

Digital Object Identifier 10.1109/ACCESS.2019.2913630

An Open Source Modeling Framework for Interdependent Energy-Transportation-Communication Infrastructure in Smart and Connected Communities

XING LU¹, KATHRYN HINKELMAN¹, YANGYANG FU¹, (Student Member, IEEE), JING WANG¹, WANGDA ZUO^{1,2}, QIANQIAN ZHANG³, (Student Member, IEEE), AND WALID SAAD³, (Fellow, IEEE)

¹Department of Civil, Environmental and Architectural Engineering, University of Colorado, Boulder, CO 80309, USA

²National Renewable Energy Laboratory, Golden, CO 80401, USA

³Wireless@VT, Electrical and Computer Engineering Department, Virginia Tech, Blacksburg, VA 24061, USA

Corresponding author: Wangda Zuo (wangda.zuo@colorado.edu)

This work was supported by the National Science Foundation through the BIGDATA Collaborative Research: IA: Big Data Analytics for Optimized Planning of Smart, Sustainable, and Connected Communities under Award IIS-1802017 and Award IIS-1633363.

ABSTRACT Infrastructure in future smart and connected communities is envisioned as an aggregate of public services, including energy, transportation, and communication systems, all intertwined with each other. The intrinsic interdependency among these systems may exert the underlying influence on both design and operation of the heterogeneous infrastructures. However, few prior studies have tapped into the interdependency among these systems in order to quantify their potential impacts during standard operation. In response to this, this paper proposes an open-source, flexible, integrated modeling framework suitable for designing coupled energy, transportation, and communication systems and for assessing the impact of their interdependencies. First, a novel multi-level, multi-layer, multi-agent approach is proposed to enable flexible modeling of the interconnected systems. Then, for the framework's proof of concept, preliminary component and system-level models for different systems are designed and implemented using Modelica, an equation-based object-oriented modeling language. Finally, three case studies of gradually increasing complexity are presented (energy, energy + transportation, and energy + transportation + communication) to evaluate the interdependencies among the three systems. Quantitative analyses show that the deviation of the average velocity on the road can be 10.5% and the deviation of the power drawn from the grid can be 7% with or without considering the transportation and communication system at the peak commute time, indicating the presence of notable interdependencies. The proposed modeling framework also has the potential to be further extended for various modeling purposes and use cases, such as dynamic modeling and optimization, resilience analysis, and integrated decision making in future connected communities.

INDEX TERMS Communities, interconnected systems, Modelica, modeling, multi-infrastructure systems, object oriented methods, open source software.

I. INTRODUCTION

Urbanization has become a mega-trend in the world today [1]. The resulting large population in urban communities will exert tremendous pressure on existing infrastructure. To mitigate this issue, the concept of smart and connected communities has recently been proposed in which new and green technologies are embraced collectively to deliver essential services, including power, mobility, and connection [2].

The associate editor coordinating the review of this manuscript and approving it for publication was Giambattista Gruosso.

Fig. 1 shows our vision of future smart and connected communities. These connected communities will include three key infrastructure systems: energy, transportation, and communication infrastructure. The energy system includes different heterogeneous components such as increasing renewable energy resources, buildings as virtual batteries, as well as massive adoption of electric vehicles (EVs). The transportation system is also expected to undergo an unprecedented evolution due to the shift toward full electrification and autonomous vehicles [3]–[5]. The communication system will become an indispensable enabler to

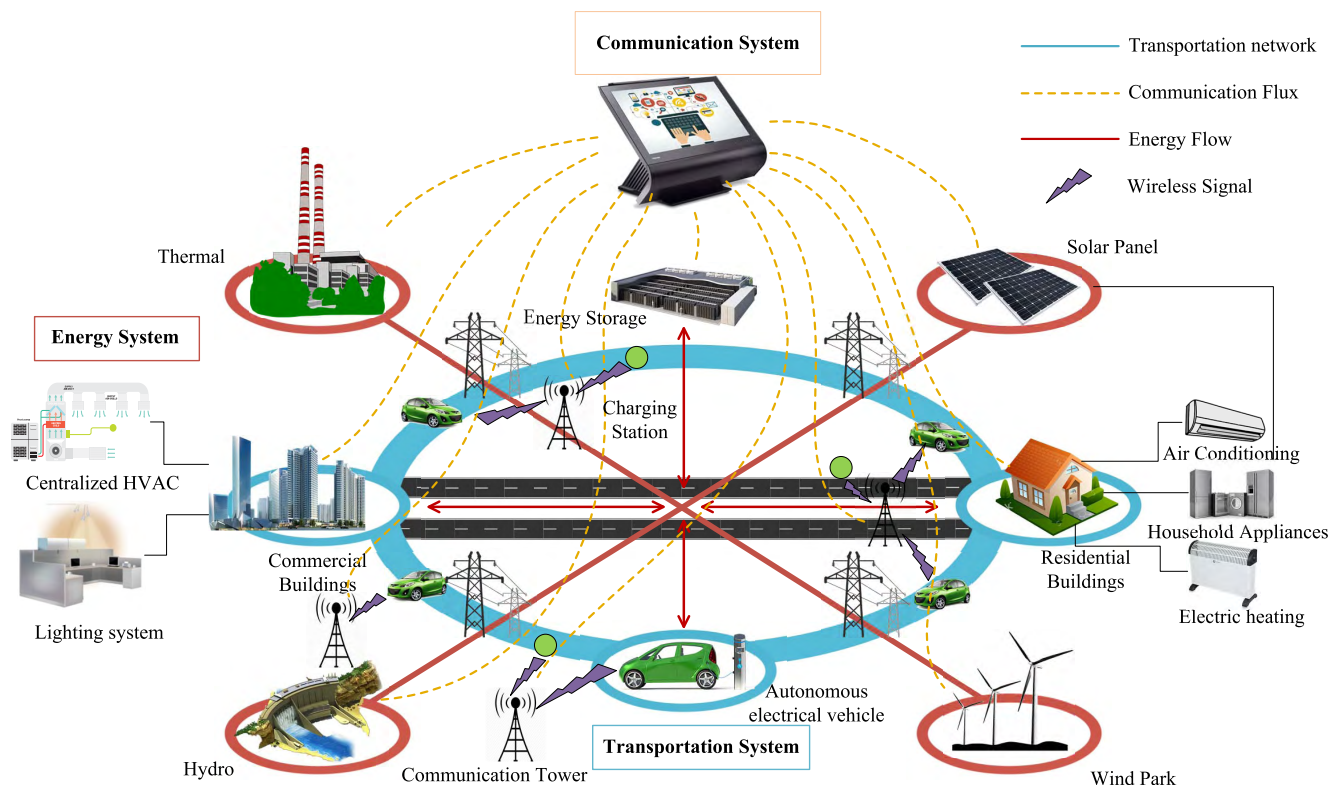


FIGURE 1. A vision of different infrastructure systems in future connected communities.

support the aforementioned infrastructure systems, link various system components, and coordinate the operational sequences [6], [7].

Infrastructure interdependency involves a bidirectional relationship between systems in which the state of each system is dependent on and intertwined with the other. For a simple example, communication networks need power from the electric grid to function, while the electric grid needs the communication networks to dispatch generation facilities according to the demands. With these codependent relationships, disturbances and capacity stresses on one system can affect the other, potentially creating a cascading effect that compromises the systems’ operations.

Today, these interdependencies are most often felt in critical infrastructure systems (CIS) – which include energy, transportation, and communication systems, among many others. It is well proven that CIS are indeed highly intertwined and codependent [8]–[10]. In the future, increased electrification and connectivity will further complicate these interconnections, as demonstrated in Fig. 1. To date, interdependency modeling primarily focuses on averting potentially catastrophic failures and minimizing the risks of future failures. This is justly so; while these interdependencies today often go unnoticed in their typical operation, they effectively aggravate and compound system failures when subjected to various stresses (such as cyber attacks, congestion, and natural disasters). In the near future, it is likely that infrastructure

vulnerabilities will become increasingly present in day-to-day operations due to their deeply crosslinked nature.

Due to the inherent complexities in future SCC infrastructure, we reorganize the sophisticated and elusive relationships in Fig. 1 into Fig. 2, which illustrates the interaction among the different systems considered. The interdependencies exist both within and between systems and present themselves on several levels, which are commonly classified under four types: (1) physical, meaning the state of one system depends on the material output(s) of the other, and vice versa; (2) cyber, meaning there is information exchange between the systems; (3) geographic, meaning the infrastructure components are in close spatial proximity with each other; and (4) logical, meaning there is a different mechanism (e.g. policy, legal, or regulatory regime) that logically ties the infrastructure systems. A physical interdependency example is in the electricity exchange between transportation and energy systems, where EVs take electricity from the grid while charging, but they can provide ancillary services with their large storage capacities and quick discharging abilities [11]. Further, a logical interdependency arises when the utility company increases the electricity price due to rising charging demand, which in turn affects the drivers’ charging patterns and the traffic condition [12]. On the cyber level, the quality of the supporting communication services affects the transportation and energy systems (shown as the dashed lines). In the transportation system, communication services

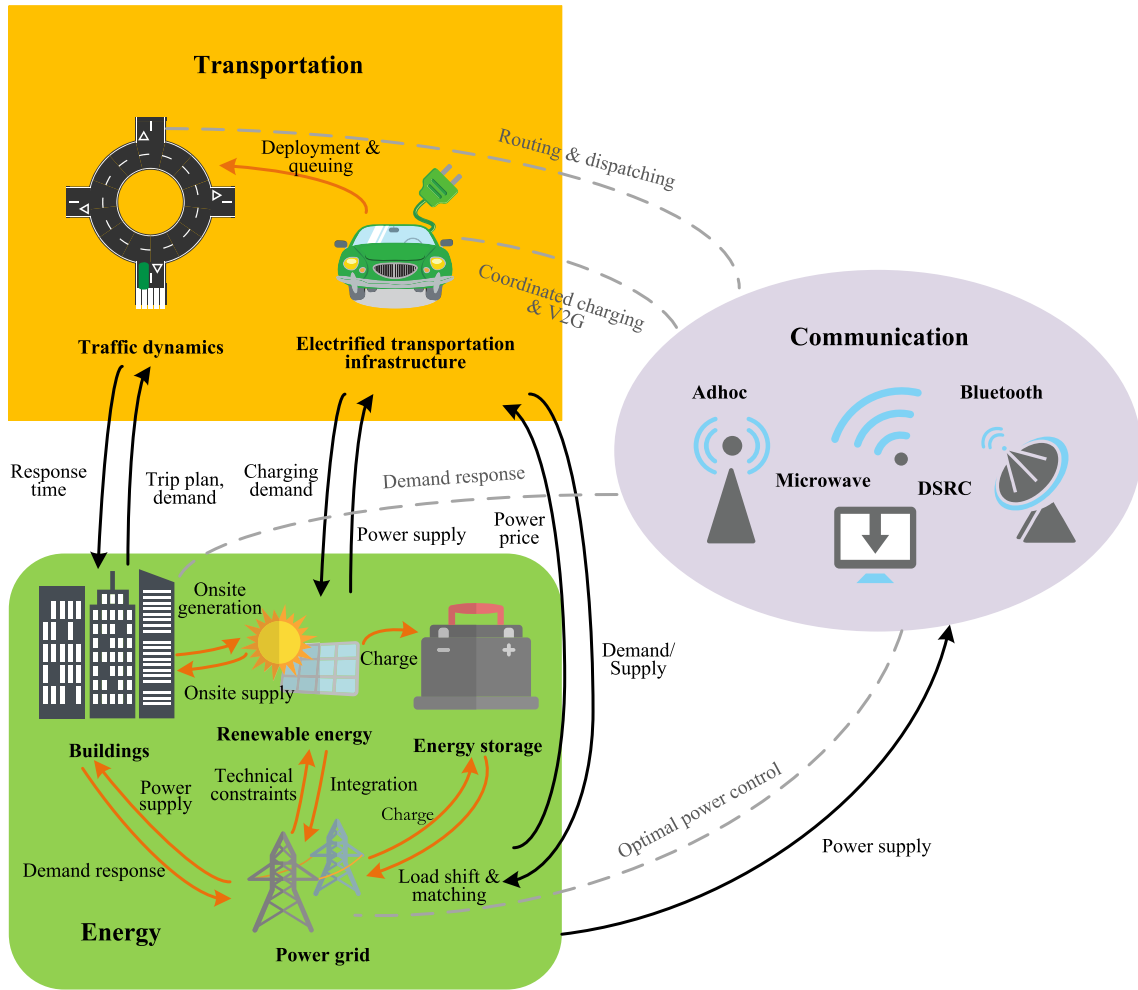


FIGURE 2. A schematic of the interdependent infrastructure systems in connected communities.

enable vehicle routing, dispatching, coordinated charging, and the implementation of vehicle-to-grid interaction. These interdependencies indicate a need to consider multiple infrastructure systems when operating future SCCs. To this end, modeling and simulation is an effective method where these complex, multilevel interactions among several infrastructure systems can be studied [13].

A. PRIOR WORKS

One cost-effective way to evaluate the integrated infrastructure systems in a connected community is through computer-aided modeling. The existing community modeling approaches can be grouped into two types: discipline-specific modeling and integrated modeling. The discipline-specific modeling of community infrastructures has been well-developed over the past decades and numerically dedicated to particular purposes of urban building energy modeling [14]–[17], urban mobility modeling [18]–[22], and communication network simulation [23]–[25]. Urban building energy models are targeted at predicting the energy use in a community, which is a relatively nascent field [14]. For the

urban mobility simulation, Multi-Agent Transport Simulation (MATSim), Simulation of Urban Mobility (SUMO), and Transportation Analysis and Simulation System are the three mainstream, open source simulators to conduct transportation analysis and dynamic traffic assignment [26]. In the context of communication network modeling in the interconnected infrastructure systems, ns2/ns3 [23] and OMNeT++ [24] are widely used due to their open source nature. Although the discipline-specific modeling can provide accurate and efficient results for the phenomenon of interest, its functionality deteriorates when it comes to the interdependent infrastructure systems due to significant simplifications [27].

In contrast, integrated modeling approaches are more suited for the interdependent infrastructure systems. Several modeling techniques have been adopted, including agent-based modeling, input-output models, network based approaches, and system dynamics. Some recent works [28], [29] considered mathematical modeling of interdependent infrastructure; however, these simplified numerical simulations have limited capabilities in modeling real-world SCCs. To achieve a higher fidelity, specialized

TABLE 1. State-of-the-art of integrated models for energy, transportation, and communication infrastructure.

Energy & Transportation				
Model name	Simulation tools		Use cases	Open Source
	Energy	Transportation		
NA [36]	In-house codes		Power flow and travel cost optimization	Unknown
NA [37]	In-house codes		Transportation-energy nexus assessment	Unknown
NA [38]	OpenDSS	DYNASMART	Impact of EVs at the distribution feeder level	Unknown
NA [51]	MATPower	Clean Mobility Simulator	Power system safety; transportation performance assessment	Full
NA [52]	DigSILENT PowerFactory	MATSim, EVSim	Charging strategy assessment; V2G	Partial
NA [53]	EMTP-rv	SUMO	Charging strategy assessment; Complex network planning	Partial
Energy & Communication				
Model name	Simulation tools		Use cases	Open Source
	Energy	Communication		
EPOCHS [39]	PSCAD, PSLF	ns-2	Multi-agent protection and control systems	Partial
INSPIRE [40]	PowerFactory	OPNET	Wide-area monitoring, protection, and control (WAMPAC) in high voltage grid	Partial
VirGIL [41]	Energyplus, Dymola, DigSILENT PowerFactory	OMNeT++	Demand response; Vol/var control	Partial
Gridspice [54]	GridLab-D, MATPOWER	Simplified	Transmission and distribution system; Demand side management/Demand response	Partial
NA [55]	PSCAD/EMTDC	OPNET	WAMPAC in high voltage grid	Partial
NA [56]	Simulink, JADE	OMNeT++	WAMPAC in middle voltage grid	Partial
Transportation & Communication				
Model name	Simulation tools		Use cases	Open Source
	Transportation	Communication		
Veins [42]	SUMO	OMNeT++	Inter-vehicular communications performance evaluation	Full
VNS [43]	DIVERT 2.0	ns-3	Inter-vehicular communications performance evaluation	Full
HINT [44]	SUMO	ns-3	Traffic management scenario analysis	Full
VSimRTI [45]	SUMO/VISSIM	OMNeT++, ns-3	Dynamic traffic flow simulation	Partial
iTETRIS [57]	SUMO	OMNeT++	Largescale vehicular network simulation	Full
NA [58], [59]	In-house codes		Vehicle routing algorithm analysis	Unknown

NA: Not applicable; **Partial:** Partial simulators are open source; **Full:** All the simulators are open source; **Unknown:** The open source status is unknown.

software packages that use validated model libraries and tailor-made solvers are coupled by a certain orchestration mechanism. Table 1 shows a non-exhaustive list of the references that model energy, transportation, and communication systems and their interdependencies. Details in terms of the platforms, simulators, use cases, and open source statuses are also included.

For SCC applications, most of the related works have focused on the integration of two systems and utilized proprietary integrated modeling tools. Coupling the energy and transportation systems, Farid [37] proposed a modeling framework using graph theory and petri-net models to assess the effects of transportation-electrification. Su *et al.* [38] coupled the OpenDSS and DYNASMART to evaluate the potential impacts of electric vehicle charging at the feeder level. However, these studies do not simulate the detailed communication processes and control management, in which the energy, transportation, and communication systems are coupled. For the energy and communication systems, profound efforts have been made to couple continuous power system simulators with discrete communication network simulators. The typical simulation platforms include the electric power and communication synchronizing simulator (EPOCHS) [39]

and the integrated co-simulation of power and information and communications technology (ICT) systems for real-time evaluation (INSPIRE) [40]. A recent coupled platform built by Chatzivasileiadis *et al.* [41] implemented the Ptolemy II framework to integrate the building models, power system software, and the communication network software. The platform can be used to investigate demand-response strategies and voltage control strategies. For the transportation and communication systems, a traffic simulator is used to understand traffic patterns and to reduce real-life traffic congestion. Conversely, network simulators concentrate on network states and events such as routers, mobile nodes, and transmission rates. The combined modeling of transportation and communication systems can be utilized in the analysis of inter-vehicular communication performance [42], [43], traffic management scenario [36], [44], and dynamic traffic flow [45].

While most existing research focuses on integrating two systems, Bedogni *et al.* [46] integrated three systems (a mobility simulator, a dynamic power distribution network simulator, and a UMTS communication network simulator). However, the scalability of their coupled model is limited, and their proposed model is dedicated to the power control of EV charging stations. The rigid coupling approach adopted

in their study blocks the model itself from adapting other scenarios that are common in the context of SCCs infrastructure systems.

Beyond SCC applications, the state-of-the-art approaches in CIS modeling are well summarized in the existing literature [10], [30]. Many successful projects have modeled the interdependencies among CIS. For example, several groups [31]–[34] proposed different cascading failure models for interdependent power and communication networks. Similarly, Heracleous *et al.* [35] developed hybrid automata models for the interdependent power, water, and communication infrastructures. While related, interdependency modeling for CIS may not be extensible to study SCCs during typical operation. Interdependent CIS models are often built to understand how these complex, interdependent systems will respond to disruptions and changing conditions. As such, their simulation goal is not to produce an “exact” outcome, but to illustrate possible outcomes to inform urban planning and design. By contrast, the underlying dynamics and model fidelity are crucial in the SCC modeling case, where the intention is to study use cases for typical operation.

The above literature review demonstrates that discipline-specific modeling for SCCs usually specializes in an isolated system and simplifies or even neglects the interdependencies among other systems. Meanwhile, integrated modeling does consider the interdependencies; however, the existing models are often limited by their proprietary nature and two-system focus. Furthermore, interdependency modeling in CIS applications is well developed but may not be fully extendable to studying SCC operational cases. Therefore, it is important to have an open source modeling framework that can cover different operational scenarios of the entire infrastructure. This is particularly important because the reactions to events in a single system may spread across multiple systems due to the interdependencies present [47].

B. CONTRIBUTIONS

In response to the aforementioned limitations of current modeling of infrastructure systems, the main contribution of this paper is to develop an open source, flexible, and extensible modeling framework for studying interdependent energy, transportation, and communication infrastructures during typical SCC operation. The open source model can be found at <https://www.colorado.edu/lab/sbs/scc-library>. We propose a novel multi-level, multi-layer, multi-agent approach to enable flexible modeling of the three interconnected systems of energy, transportation, and communication. The proposed framework is then implemented on Modelica-based modeling platforms [48]–[50], which provides important features like objected-oriented, acausal modeling and equation-based schemes. In addition, we develop various component and system-level models for energy, transportation, and communication systems. The objective of these models is to demonstrate the application of the proposed framework; therefore, the interdependency and system models are selected to adequately test the framework while minimizing complexities at

the current stage. To the best of our knowledge, this is one of the first attempts to couple all the three energy, transportation, and communication systems in a flexible and scalable way to evaluate and quantify the underlying interdependencies of their infrastructures for SCCs.

The rest of the paper is organized as follows. Section II presents the proposed smart community modeling framework based on the multi-level, multi-layer, multi-agent (3M) approach for coupling multiple infrastructure systems. Section III introduces the Modelica implementation of the proposed modeling framework as well as various component and system models in Modelica. Section IV presents three case studies to demonstrate the application scenarios of the modeling framework and the measurable interrelations among the three systems. Finally, concluding remarks are presented in Section V.

II. MULTI-LAYER, MULTI-BLOCK, MULTI-AGENT APPROACH

This study proposes a 3M approach for the flexible and extensible modeling of the coupled systems in a community level. This generalized modeling approach can be adapted to different scenarios and use cases in the design and operation of SCCs. The modular nature of the 3M approach allows various system combinations to be studied (two-system models, three-system model, and so forth). Furthermore, the generalized, adaptable framework can readily accept a variety of other component models along with their dependency interconnections to evaluate many dynamic systems. In this section, we use the three-coupled system to illustrate the modeling approach.

Fig. 3 illustrates the principle of the proposed 3M approach. The multi-layer represents a hierarchical structure, which consists of a community layer, a block layer, and a system agent layer from the top level to the bottom. At the community layer, the entire community will be divided into several functional blocks, such as residential blocks, commercial blocks, industrial blocks, or mixed-functional blocks. It could also be divided according to domain-specific entities, such as distinct power distribution networks. The block layer has three system agents for the energy, transportation, and communication systems. Different infrastructure systems should be mapped accordingly in one block. Within each system agent (system agent level), there will be individual subagents for infrastructure nodes. For instance, an energy system agent could have subagents for renewable generation, batteries, and utility customers. Likewise, the transportation system agent could have subagents for connected roads, charging stations, and vehicles. The communication system agent could consist of different communication devices (control centers, backbone routers) according to the different types of communication networks (e.g. cellular/LTE, Wi-Fi, or PLC).

We next illustrate the interdependencies and data exchange between these agents and blocks in a bottom-up fashion. At the system agent layer, multiple agents could exchange data

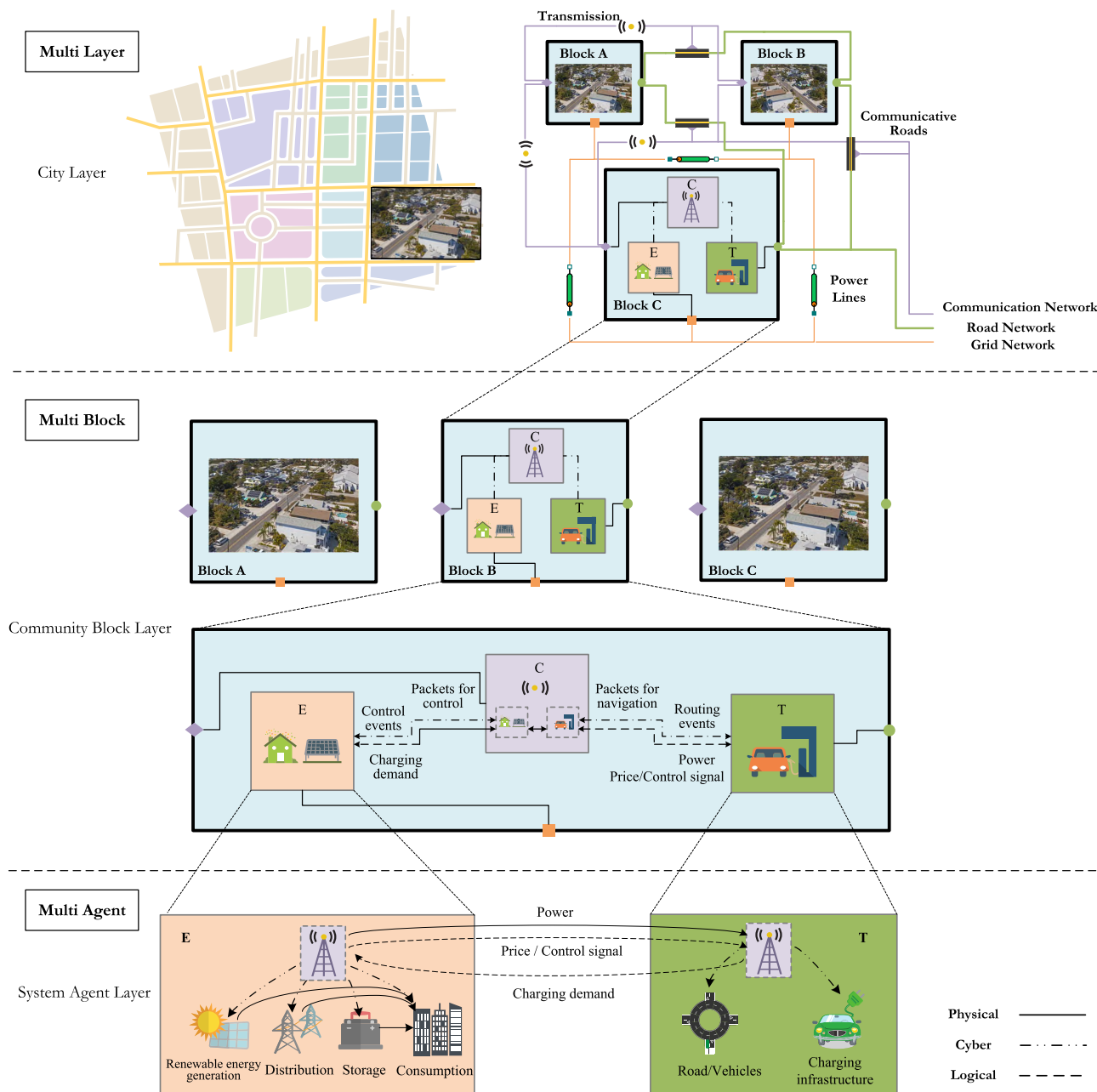


FIGURE 3. A schematic of the 3M approach for modeling coupled systems.

through certain interfaces. As shown in Fig. 3, the interdependencies can be physical, cyber, or logical, and both internal and external dependencies are present. In the energy domain, the different components will communicate with each other to achieve stable and economic operations of the power grid. For example, in a demand response application, the electricity demand of each customer can be properly rescheduled via the communication network to reduce the peak demand between the power grid and its customers. While in the transportation domain, different components will also interact with

each other to achieve a good traffic condition. For example, the queuing and power availability information in the charging stations and the routing information could be broadcast to the vehicles for optimal routing and charging arrangements. The aforementioned connections are the inner data exchanges in each domain. To ensure a collective optimal operation of the energy and transportation domains, the agents from the energy system will calculate the electricity price under different load profiles and trigger the necessary power controls of the charging stations. In response to this, the transportation

agents will calculate the traffic condition, decide the routing and charging behavior of electric vehicles, and determine the charging load of each charging station node. In this system agent layer, we could select the needed component model according to the use cases.

At the block layer, we encapsulate all the component models from the system agent layer and merge the different communication centers into one communication system agent, which would calculate the communication latency among the different components. The generalized data exchange between different system agents are propagated from the data exchange in the system agent layer. The energy system agent will transfer power from the grid to charge the EVs (physical) and send the packets for the power system control through the communication system agent (cyber). The communication simulators within the communication system agent will then return the control events (cyber) to the energy system agent. Likewise, the transportation system agent will send the packets for navigation purpose to the communication system agent (cyber), and it will receive the routing events from the communication system agent (cyber). Lastly, the energy system and transportation system agents will exchange the control/price signal and the charging demand via the communication agent (logical). Note that the aforementioned generalized dependencies could be specialized by different use cases, which should be aligned with the system agent layer.

In the community layer, the different blocks are linked with each other through the corresponding ports. The power port links the energy system agents in different blocks to a power grid network, and the traffic port links the transportation system agents in different blocks to a road network. The communication system agents will communicate in a larger network, and the information will be collected and scattered in a large scale communication center or in distributed hubs. In future SCCs, the roads and the power lines could also be a communicative component in this layer.

The proposed 3M approach allows the flexible and extensible modeling of multiple infrastructures. The modeler could save efforts by using this standardized and generalized approach since the interfaces and the data exchange ports from the upper layer are fixed. As such, only the component models in the lower layer require designing and refinement. The proposed modeling framework facilitates the model reuse and can be used to investigate different use cases in the design and operation of SCCs. In the next section, we will introduce our efforts to designing and modeling preliminary multi-infrastructure systems in order to test and validate the 3M approach.

III. MODEL DESCRIPTION AND IMPLEMENTATION

Using the proposed 3M approach, we implement the coupled models in Modelica, an object-oriented modeling language. Section III-A illustrates the implementation of system agent models of the energy, transportation, and communication systems. Sections III-B and III-C discuss the implementation of block layer and community layer models, respectively.

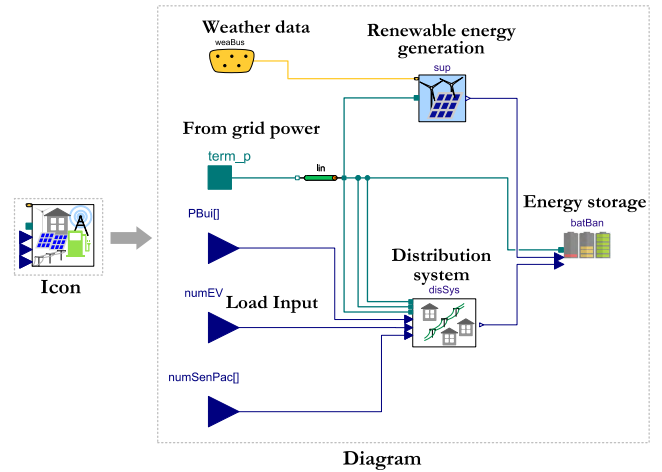


FIGURE 4. Implementation of the energy system models in Modelica.

A. SYSTEM AGENT MODEL

1) ENERGY SYSTEM

The energy system is composed of renewable generation equipment (e.g. photovoltaic (PV) panels and wind turbines), energy storage devices, power draw from the grid, and distribution systems. The feeders of the distribution system connect various types of loads, such as the load from buildings, EVs, communication towers, and general loads in the power grid. Fig. 4 shows the Modelica implementation of the energy system. The following subsections describe the detailed description and implementation of different energy component models.

a: RENEWABLE ENERGY GENERATION

In this paper, we assume renewable energy generation consists of energy supplied from PV and wind turbines. The PV system is modeled with the *PVSimpleOriented* model in the Modelica Buildings Library. The total aggregated electrical power P_{PV} generated by the PV systems is represented by:

$$P_{PV} = \sum_{k=1}^{N_{PV}} (A_k \cdot f_{act,k} \cdot \eta_k \cdot G_k \cdot \eta_{DCAC,k}) \quad (1)$$

where N_{PV} is the total number of PV arrays, A is the area of each PV array, f_{act} is the fraction of the aperture area, η is the PV efficiency, G is the total solar irradiation, and η_{DCAC} is the efficiency of the conversion between direct current (DC) and alternating current (AC). In this model, G is the sum of direct irradiation G_{Dir} and diffuse irradiation G_{Dif} :

$$G = G_{Dir} + G_{Dif} \quad (2)$$

$$G_{Dir} = \max(0, \cos(\theta)) \cdot H_{DirNor} \quad (3)$$

$$G_{Dif} = G_{SkyDif} + G_{GroDif} \quad (4)$$

where θ is the solar incidence angle on the surface, and H_{DirNor} is the direct normal radiation. G_{SkyDif} and G_{GroDif} are the hemispherical diffuse solar irradiation on a tilted surface from the sky and the ground, respectively.

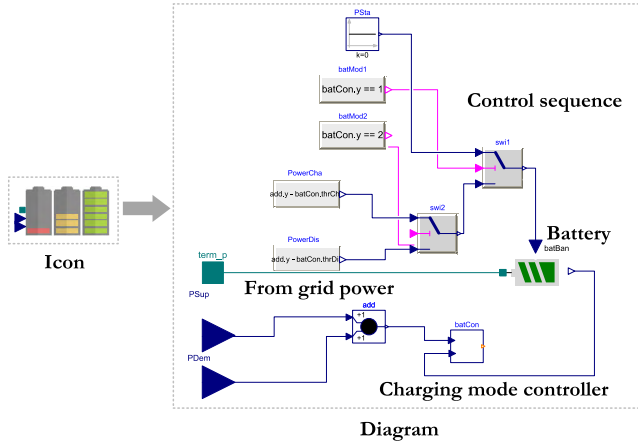


FIGURE 5. Diagram of Modelica models for energy storage and its control logic.

The *WindTurbine* model in the Buildings library is adopted for wind turbines. For a single turbine, the model computes generated power P_t as a function of the wind speed. The aggregated active electrical power generated by all the wind turbines P_{win} is calculated as:

$$P_{win} = \sum_{k=1}^{N_{win}} (P_{t,k} \cdot scale_k \cdot \eta_{DCAC_win,k}) \quad (5)$$

where *scale* is used to scale the wind power generation based on the P_t ; N_{win} is the total number of wind turbines; and η_{DCAC_win} is the rate of conversion from DC to AC.

b: ENERGY STORAGE

A new energy storage model is built based on the *Electrical.AC.OnePhase.Sources.Battery* model in the Buildings library, since the base model does not enforce that the state of charge is between zero and one. The new model provides a control sequence such that only a reasonable amount of power is exchanged. The new model and corresponding control sequence are shown in Fig. 5. The control logic here is that the power generated by the renewable system covers the demand load in the first place. When there is excessive power, the battery starts to charge. When the power demand exceeds a certain threshold, the battery starts to discharge. In other cases, the battery remains stand-by.

c: POWER DISTRIBUTION NETWORK

Different configurations of power distribution networks are built in the energy system agent model. These networks can be used to investigate the performance of power distribution systems. Fig. 6 shows the IEEE 16-node test feeder configuration [60] and its implementation in Modelica.

Different types of loads (buildings, EVs, general, and communication components) are connected to the feeders. The loads from buildings can be calculated using grey-box models such as RC models [61] or imported by data-driven models [62]. The aggregated EV charging power P_{EV} is

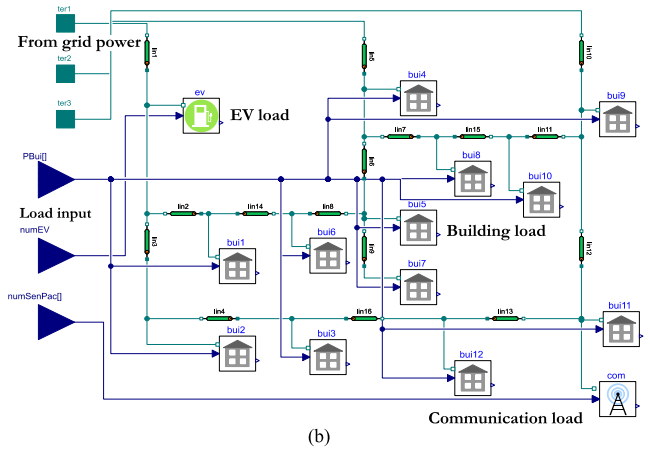
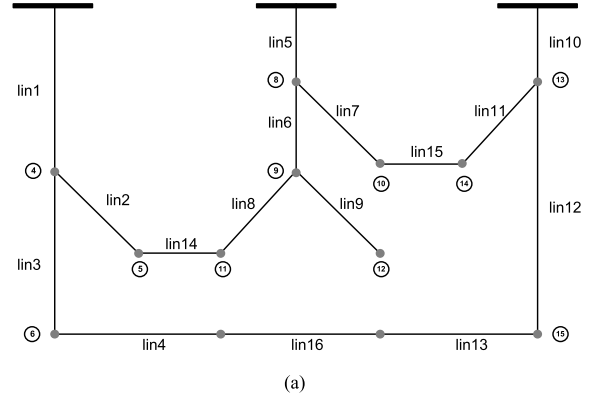


FIGURE 6. The IEEE 16-node test feeder configuration: (a) System schematic and (b) Modelica Implementation.

calculated as follows:

$$P_{EV} = \sum_{k=1}^{N_{char}} P_{char,k} \quad (6)$$

where N_{char} is the total number of the charging EVs in (12), and $P_{char,k}$ is the charging power of each EV. As a demonstration case, the current paper assumes P_{char} is constant for all EVs [63]. The total load from all of the communication towers P_{com} is given by [64]:

$$P_{com} = \sum_{k=1}^{N_{com}} (2Q_{c,k} \cdot E_{elec,k} + Q_{c,k} \cdot \epsilon_{elec,k} \cdot d_k^\alpha) \quad (7)$$

where N_{com} is the number of communication towers, E_{elec} is the equipment power for sending and receiving packets, Q_c is the packet throughput, d is the distance of the transmission, and α and ϵ_{elec} are transmission coefficients.

d: POWER DRAW FROM THE GRID

We use the *Electrical.AC.OnePhase.Sources.Grid* model in the Buildings library to create the physics-based model for the utility supplied power [65]. The input for this model is a fixed voltage signal while the output is the power supplied by the utility to the power distribution system. The convention is

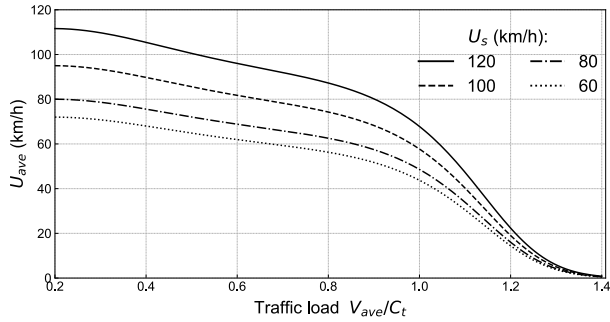


FIGURE 7. Empirical model of traffic flow-velocity correlation for a certain road [68].

that the power is positive if real power is consumed from the grid and negative if power flows back into the grid.

2) TRANSPORTATION SYSTEM

Traffic flow is intrinsically non-reproducible; it is therefore impossible to predict precise vehicle trajectories via models. However, it is recognized that the prediction of large-scale field quantities can be possible [66]. The traffic simulation models can be micro-, meso- and macroscopic with different granularities [67]. For example, macroscopic models describe the traffic as flows, velocities, and densities of vehicles, while microscopic models simulate individual vehicles down to basic physical and kinematic properties such as speed, locations, and fuel. In this research, we simulate transportation infrastructure from a macroscopic perspective. The road and charging station models are detailed in this section.

a: ROAD MODEL

The road model described here is able to model traffic outflow given the traffic inflow profile of a road, which utilizes the empirical flow-velocity correlation from literature [68], [69], as shown in (8):

$$\begin{cases} U_{ave} = \frac{\alpha_1 \cdot U_s}{1 + (\frac{V_{ave}}{C_t})^\beta} \\ \beta = \alpha_2 + \alpha_3 \cdot (\frac{V_{ave}}{C_t})^3 \end{cases} \quad (8)$$

where U_{ave} is the average road velocity; V_{ave} is the average vehicle flow; C_t is the road capacity; α_1 , α_2 , α_3 , and β are regression parameters; and U_s is the speed designed for the road. The traffic of the road can be measured by the traffic load $\frac{V_{ave}}{C_t}$. Fig. 7 demonstrates the relationship between U_{ave} and $\frac{V_{ave}}{C_t}$ of different U_s limits under a certain road type. We can then find that the velocity descends faster when traffic flow exceeds the road capacity ($\frac{V_{ave}}{C_t} > 1$).

Equation (9) represents the relationship between the velocity, density, and traffic flow:

$$V_{ave} = \frac{U_{ave} \cdot \int (q_{out} - q_{in}) dt}{L} \quad (9)$$

where q_{out} and q_{in} are respectively the traffic outflow and traffic inflow rates, and L is the length of the road.

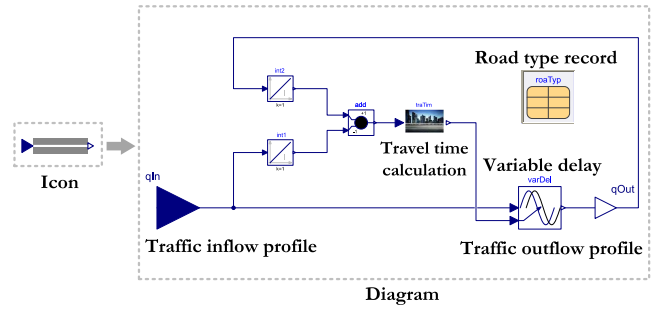


FIGURE 8. Diagram of Modelica models for roads.

```

...
equation
num=qIn; //Traffic inflow
qAve=num/l*u; //Average traffic flow on the road
b=roaTyp.a2 + roaTyp.a3*(qAve/(roaTyp.q_nominal/3600))^3; //Beta
u=roaTyp.a1*roaTyp.uf/(1+(qAve/(roaTyp.q_nominal/3600))^b); //Average velocity
t=if noEvent(u>0.1) then l/u else l/0.1;
delTim=t; //Travel time

```

FIGURE 9. Pseudo-code of *traTim* model in Modelica.

Equation (10) represents the travel time on the road:

$$t_{w/oCom} = \frac{L}{U_{ave}} \quad (10)$$

where $t_{w/oCom}$ is the travel time of the road without considering the communication system. Combining (8)-(10), the traffic condition on the road can be jointly obtained. In our Modelica implementation, the road model consists of the *traTim* model and the *varDel* model (see Fig. 8). The pseudo-code of the *traTim* model using the aforementioned principle is shown in Fig. 9. Based on the aforementioned principles, the *traTim* model is built to calculate the travel time of the road section. The *varDel* model is a delay block to mimic the travel delay time due to traffic conditions. Different road properties could be selected from the road type record datasets.

b: CHARGING EV NUMBER MODEL

The number of EVs in the community is calculated using a traffic flow balance:

$$\dot{N} = \sum_{k=1}^{m_{in}} q_{in,k} - \sum_{k=1}^{m_{out}} q_{out,k} \quad (11)$$

where \dot{N} represents the change of the number of EVs parked in the block; m_{in} and m_{out} denote the number of inlets and outlets of the station, respectively; and q_{in} and q_{out} represent the traffic inflow and outflow rates, respectively. While we recognize the number of vehicles is an integer in reality, we assume N is continuous in this preliminary implementation. The pseudo-code of the model using the aforementioned principle is shown in Fig. 10.

There are many ways we can estimate the EV charging in the block level. In this case study, we use a simplified probabilistic model. For one single EV, its probability of charging

```

...
equation
qOut[:]=qOutSet[:]; //Prescribe traffic flow at the outlet
der(numEV)= (sum(qIn[:])-sum(qOut[:]))/3600;
//Charging EV number balance

```

FIGURE 10. Modelica pseudo-code for the number of charging EVs.

at the block at a given hour is p_i , which can be obtained by survey data. We assume the number of the charging EVs at certain time represents a Poisson distribution. Therefore, we expect:

$$N_{\text{char}} = E(M) = p_i \cdot N \quad (12)$$

where N_{char} is the total number of the charging vehicles, as discussed in (6), and N is number of parked vehicles in the block per (11). For later applications, this simplified model can be replaced with more accurate and realistic models, such as Monte Carlo models [70].

3) COMMUNICATION SYSTEM

In this preliminary case study, a simplified packet loss model is used to describe the transmission process in a wireless communication network [71]. The empirical relationship between the packet loss rate γ and the normalized throughput Q_c is:

$$\gamma = \kappa \cdot \sqrt{Q_c - C_c} \quad (13)$$

where κ is a proportional coefficient and C_c is the threshold of the transmission. We assume that γ is directly proportional to Q_c under certain bandwidth in the communication system. In this simplified model, we assume the transmission delay Del equals 0 that there are negligible impacts from the re-transmission mechanism if a message is lost.

4) COMPONENT VALIDATION

We validated the models using comparative testing and analytical verification. For example, comparative testing is used to validate the road model, which compares the Modelica simulation results with the data mentioned in literature [72]; this includes the flow rate data from the inlet to the outlet marked at 15 minute intervals for 6 hours. The detailed comparison can be seen in Fig. 11. From this, we can conclude that the model fits well with the literature data and could represent the traffic condition for the integrated model.

B. BLOCK LAYER MODEL

The block layer model reflects the interaction of the different system agents in a block, as mathematically illustrated in (14)-(18). The interdependent variables, shown in bold, exemplify how the outputs of one system agent are inputs of the others. They are calculated using the system agent models as shown in Section III-A.

$$\begin{aligned} \dot{S}_{E_1}(\mathbf{LMP}^i, \mathbf{Sig}_E^i, V^i, I^i, \dots) \\ = f_1(\mathbf{P}_{EV}^i, \mathbf{P}_{com}^i, P_{bui}^i, P_{PV}^i, P_{win}^i, \dots) \end{aligned} \quad (14)$$

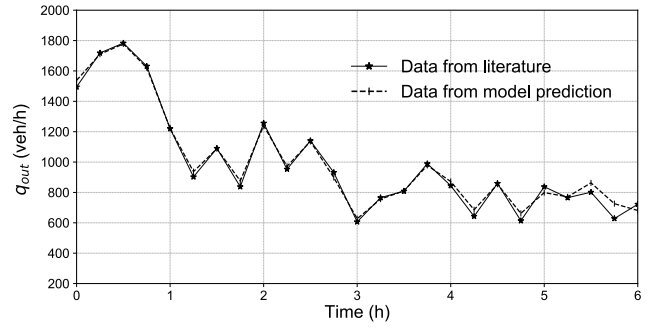


FIGURE 11. Comparison of traffic outflow from model prediction and literature.

$$\begin{aligned} \dot{S}_{E_2}(\mathbf{P}_{EV}^i, \mathbf{P}_{com}^i) \\ = f_2(N_{\text{char}}^i, Q_c, \dots) \end{aligned} \quad (15)$$

$$\begin{aligned} \dot{S}_{T_1}(N_{\text{char}}^i) \\ = g_1(q_{in}^i, q_{out}^i, \dots) \end{aligned} \quad (16)$$

$$\begin{aligned} \dot{S}_{T_2}(q_{in}^i, q_{out}^i, U^i, t_{w/Com}, \dots) \\ = g_2(C_t^i, U_s^i, LMP^i, \mathbf{Sig}_E^i, \mathbf{Sig}_T^i, Del, \dots) \end{aligned} \quad (17)$$

$$\begin{aligned} \dot{S}_C(Q_c, Del, \dots) \\ = h(\mathbf{Sig}_E^i, \mathbf{Sig}_T^i, q_{in}^i, q_{out}^i, C_c, \dots) \end{aligned} \quad (18)$$

Operator \dot{S} indicates the state variables in the energy, transportation, and communication systems, which are denoted by subscripts E , T , and C , respectively. Index i designates the node. In the energy system, the state output variables include node voltage V and line current I , as well as the locational marginal price LMP and the energy-related control signals Sig_E . These control signals include the buildings, EVs, storage, and renewable energy generations. As seen in (14), the functional inputs to \dot{S}_{E_1} include interrelated energy factors P_{EV} and P_{com} , as well as other load and renewable generation quantities – such as the building power consumption P_{bui} , P_{PV} from (1), and P_{win} from (5). Further, as shown in (15), the EV charging active power and communication tower power are determined by the number of charging EVs N_{char} in (6) and the communication throughput Q_c in (7), as mentioned in Section III-A.1.c.

As seen in (16), N_{char} correlates to traffic inflow q_{in} and traffic outflow q_{out} , as exemplified previously in (11). In the transportation system shown in (17), traffic inflow q_{in} and traffic outflow q_{out} , along with average velocity U_{ave} , road velocity U , travel time $t_{w/Com}$, are determined by the transportation parameters such as road capacity C_t , design road velocity U_s ; energy factors such as the locational marginal price LMP and electrical control signals Sig_E ; as well as communication factors such as throughput Q_c and time delay Del , as exemplified previously in (8)-(12). For reference, the empirical traffic flow model included in this paper approximates U as the average road velocity U_{ave} , as shown in (8). Further, when the communication system is considered, the transportation-related control signals Sig_T

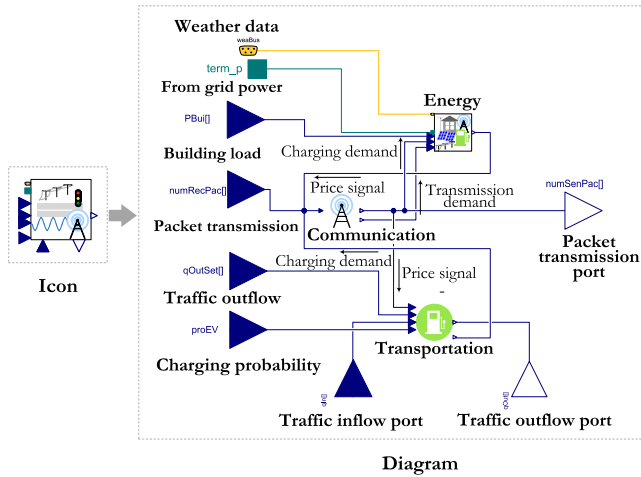


FIGURE 12. Diagram of Modelica model for one block.

affect the travel time $t_{w/Com}$, which will be elaborated further in Section III-C. In the communication system shown in (18), the throughput Q_C and time delay Del affect both the energy and transportation systems, while the transmission threshold C_c affects the communication state as prescribed in (13). The Modelica implementation of the block layer model is depicted in Fig. 12. As aligned with the block layer in the proposed 3M approach, the transportation agent sends the charging demand signal to the energy system agent via the communication agent. Likewise, the energy agent sends back the price/control signal via the communication agent.

Since the energy system supplies power to the communication system, the communication agent sends the throughput demand signal to the energy system agent so that the corresponding energy demand for the communication agent can be calculated. In this case study, the communication system in the block is also responsible for transmitting the packets for traffic routing with the interconnected roads through the packet transmission port.

C. COMMUNITY LAYER MODEL

The community layer model connects different numbers of blocks. Aligned with the 3M approach, different blocks are connected with the power lines and the communicative roads. The exemplified model shown in Fig. 13 consists of two blocks. The interdependencies on this layer are reflected by these connections of different blocks. For example, in terms of the energy connection, the voltage between the terminals at Block A and Block B is co-related by linking the terminal connectors with the power lines, which implicitly contains the following mathematical formulation:

$$V_{\phi,Block A}^p - V_{\phi,Block B}^n = Z_{tot} \cdot I_{\phi}^p, \quad (19)$$

where V , I , and Z_{tot} denote the voltage, current, and total impedance, respectively, between the terminals of Block A and Block B at phase ϕ . These correlate to (14). At the

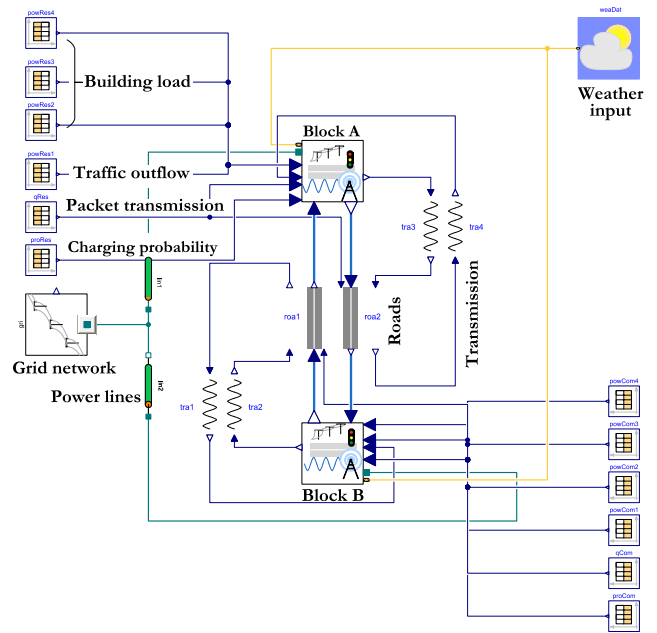


FIGURE 13. Diagram of Modelica model for a community with two connected blocks.

terminals, p and n represent the positive and negative connectors, respectively.

The communicative roads will exchange routing data with the communication centers in the block. Therefore, the performance of the packet exchanges will have an impact on the traffic conditions on the linked roads. Generically, we represent this interrelation as Sig_T in (17) and (18) above. While there are many different models to represent this correlating signal, here we adapt the packet loss rate γ to represent this signal. In the current implementation, we assume that the traffic delay time will be proportional to γ as follows:

$$t_{w/Com} = (1 + \gamma)t_{w/oCom} \quad (20)$$

where $t_{w/Com}$ and $t_{w/oCom}$ are the travel times with and without consideration of communication, respectively.

IV. CASE STUDIES

In this section, three cases are presented in which complexity is gradually added to evaluate the interdependency of different systems and the necessity of integrated modeling. Section IV-A introduces the basic information of the cases and the performance indicators used to evaluate the multidisciplinary infrastructure models. Section IV-B presents the case that only considers the energy system, while the transportation and communication parameters are fixed. The case study in Section IV-C considers both the energy and transportation system, which intends to investigate the logical interdependencies between the variable charging demand on the energy system and the traffic conditions. Lastly, the case study in Section IV-D takes the three systems into account, considering the cyber interdependencies linking the two

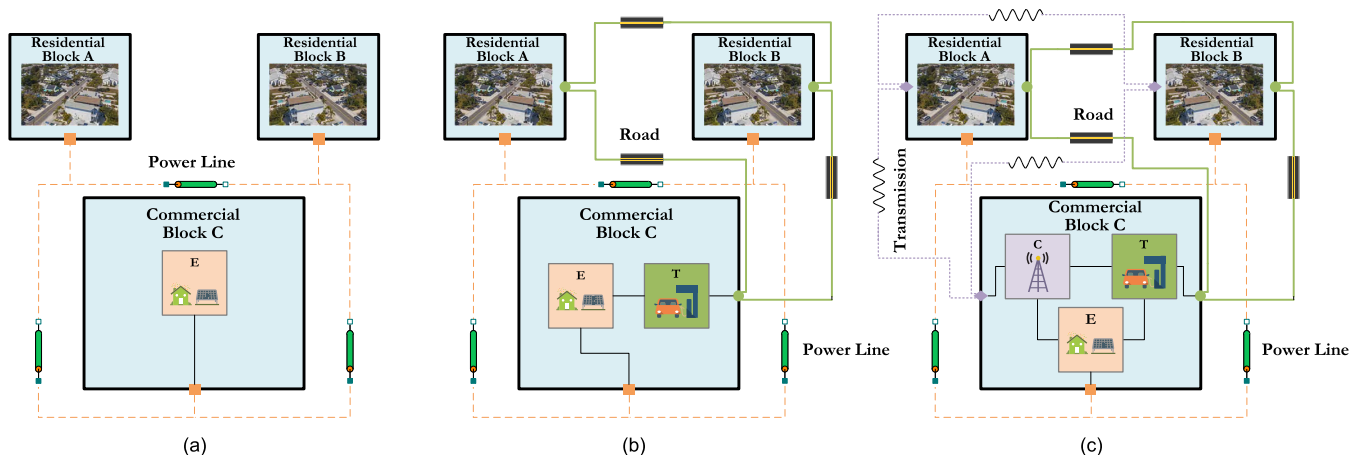


FIGURE 14. Schematics for the three cases: (a) Energy system, (b) Energy + Transportation systems, and (c) Energy + Transportation + Communication systems.

TABLE 2. Detailed model settings in the three cases.

	Residential Block 1	Residential Block 2	Commercial Block
Weather profile	San Francisco, CA, USA		
PV area (m^2)	20,000	30,000	50,000
Nominal wind turbine power (MW)	1		
Battery capacity (kWh)	4,000	5,000	6,000
Distribution system type	IEEE 16 test feeder		
Initial EV number	800	800	200
Building type	600 Residential houses	700 Residential houses	5 Large offices, 5 strip malls, 5 restaurants
Road Capacity ($C, U_s, \alpha_1, \alpha_2, \alpha_3$)	Road _{1,2} : (350, 30, 1, 1.88, 4.85) Road _{3,4} : (1100, 60, 1, 1.88, 7) Road _{5,6} : (800, 56, 1.4, 1.88, 6.97)		
Communication system coefficients (γ, C_c)	Road _{1,2} : (0.03, 80) Road _{3,4} : (0.02, 300) Road _{5,6} : (0.035, 350)		

physical systems. These examples are intended to evaluate the intertwined operational performance of energy, transportation, and communication infrastructure in connected communities where large-scale renewable energy generation and full-electrified transportation are adopted. It is noted that these preliminary models do not fully encapsulate the interdependencies present among the infrastructure systems. In the current case, the charging price is considered to be constant and the charging station control is not taken into account. As mentioned before, the objective through these case studies is to evaluate the proposed modeling framework for simulating interconnected infrastructure systems for SCC operation.

A. CASE DESCRIPTION AND PERFORMANCE MEASURES

Fig. 14 shows the schematics of the three cases. The modeled community is composed of two residential blocks and a commercial block. As the names imply, the residential blocks mainly consist of residential buildings, while the commercial block is composed of commercial buildings, such as offices, restaurants, and schools. Each block has its own renewable energy generation farm, energy storage (battery), EV charging stations, and communication towers. Six one-way roads of the

same road type link different blocks. The design capacity and design velocity vary between roads. The communication system in these cases is dedicated to the traffic routing of the vehicles on the road. The communication tower in each block exchanges traffic information with the vehicles on the road. Thus, the performance of the communication system has a direct effect on the transportation system. Detailed model settings are shown in Table 2 for the three cases.

Several indicators are selected from prior works [37], [51], [73] to assess the infrastructure performance in connected communities. The performance of energy infrastructure includes power load cover factor (*LCF*), peak-valley load ratio (*PVLR*), power system line safety, and power system voltage security. Power *LCF* evaluates the percentage of demand that can be supplied by the renewable energy generation. Power *PVLR* is one of the load balancing performance indicators in the power infrastructure, represented by:

$$PVLR = \frac{P_{max} - P_{min}}{P_{max}} \tag{21}$$

where P_{max} and P_{min} are the peak and valley power from the grid, respectively.

Power voltage security indicator, SI_B , denotes a bus voltage limit placed by the IEEE Standard 519 [73]:

$$SI_B = \frac{1}{N_b K} \sum_i^{N_b} \sum_{\kappa}^K g_i(\kappa), \text{ where}$$

$$g(i) = \begin{cases} v_{dev,i}(\kappa) - 1.05 & \text{if } v_{dev,i}(\kappa) > 1.05 \\ 0.95 - v_{dev,i}(\kappa) & \text{if } v_{dev,i}(\kappa) < 0.95 \\ 0 & \text{otherwise} \end{cases} \quad (22)$$

where $v_{dev,i}(\kappa)$ is the voltage deviation rate of a given line i and a given event κ over all events K given a set of N_b buses.

Power line safety indicator, SI_L , represents a physical rating on the amount of transferred active power:

$$SI_L = \frac{1}{N_l K} \sum_i^{N_l} \sum_{\kappa}^K f_i(\kappa), \text{ where}$$

$$f(i) = \begin{cases} P_i(\kappa) - P_i^* & \text{if } P_i(\kappa) > P_i^* \\ 0 & \text{otherwise} \end{cases} \quad (23)$$

where P_i^* is the power limit of a given line i and a given event κ over all events K given a set of N_l lines.

The performance of transportation and communication systems can be quantified by road congestion and transmission congestion, respectively. Road congestion can be gauged by the travel time and traffic flow on the road, while transmission congestion can be reflected by the packet loss or arrival rate. The detailed calculation can be seen in Sections III-A.2 and III-A.3.

B. CASE 1: ENERGY SYSTEM

The implementation of Case 1 in Modelica is shown in Fig. 15. The building loads are hourly load profiles computed using the DOE Commercial Reference Building Models [74] and Building America House Simulation Protocols [75]. The inputs for the transportation and communication systems are fixed for this case. The EV charging profile in one block is prescribed according to the travel demand analysis, and the travel time between the blocks is neglected in the simulation.

The energy-system simulation results for January 1st in San Francisco are shown in Fig. 16. From the supply side, the power generated from the PV peaks at noon. However, the wind power contributes little during the considered time period. From the demand side, the load from the EV charging has a higher demand in the night than during the daytime due to the charging pattern of the residential blocks. The load from the building blocks is quite stable compared to the EV charging load pattern. It is noted that the load from the communication towers is negligible compared to the load from EV charging and the buildings.

Regarding the power draw from the grid, the peak-valley ratio amounts to 48.79%. This relatively high value is caused by the high EV charging demand at night, which peaks at 22:20, and renewable energy generation during the daytime, which peaks at 12:10. However, the duck curve is

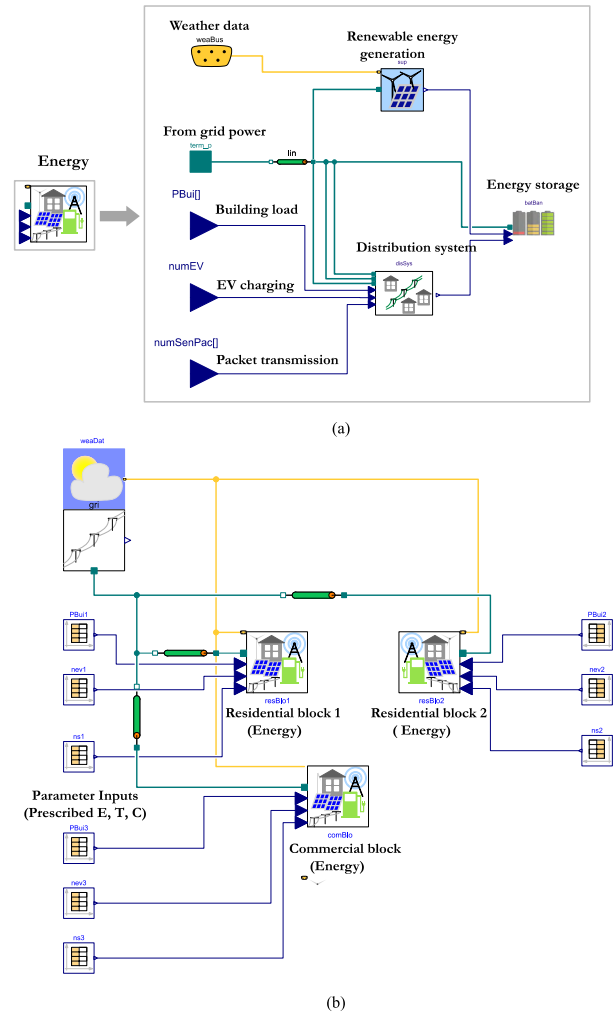


FIGURE 15. Implementation of Case 1: The (a) block icon and (b) community layer diagram for the energy system in Modelica.

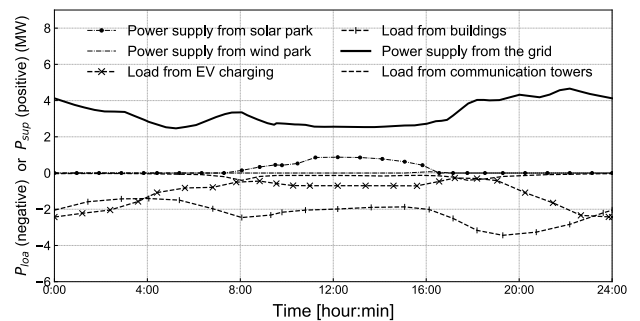


FIGURE 16. Energy system supply and demand profiles for one day in the connected community.

flattened by the adoption of the battery and the modest power load cover factor (6.92%). The overall results of the energy system indicators are listed in Table 3.

The $SI_{B,resBlo1}$ and $SI_{L,resBlo1}$ are indices for the power infrastructure performance in terms of the bus safety security and power line safety, respectively. Fig. 17 shows the line

TABLE 3. Results of the energy system indicators.

Energy system indicators			
$PVLR(\%)$	$LCF(\%)$	$SI_{B,resBlo1}$	$SI_{L,resBlo1}$
48.79	6.95	0.00766	0.0097

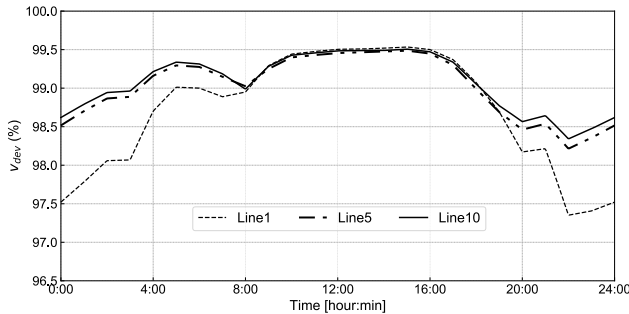


FIGURE 17. Line voltage deviation rate of three feeders at the distribution system described in Fig. 6.

voltage deviation rate of three feeders at the distribution system described in Fig. 6. These results all demonstrate that the power infrastructure has the risk of being overloaded at certain discrete time steps. These results suggest that advanced control of coordinating EV charging and building demand response should be taken to avoid the risk.

C. CASE 2: ENERGY + TRANSPORTATION (E+T) SYSTEM

The implementation of Case 2 in Modelica is shown in Fig. 18. The parameter inputs for the energy system and the communication system settings are the same as Case 1. However, instead of specifying the EV charging profile, the traffic dynamic is considered in this case based on the traffic outflow profile of the block. The traffic outflow profile is determined from the data in the National Cooperative Highway Research Program (NCHRP187) [76]. The quantitative results for the transportation system are illustrated in Fig. 19, which shows the average traffic flow profile and the average velocity on different roads. The results demonstrate traffic peaks on Road 3 and Road 6 that link the residential blocks and commercial blocks.

Meanwhile, the average traffic flow on Road 1, which links the two residential blocks, fluctuates less. At peak commute times (around 8:00 and 18:00), the average traffic flow has a peak value while the average velocity on the road has a minimum value, as can be expected. The comparison of the energy results in Case 1 and Case 2 will be analyzed in Section IV-C.

D. CASE 3: ENERGY + TRANSPORTATION + COMMUNICATION (E+T+C) SYSTEM

The implementation of Case 3 in Modelica is shown in Fig. 20. In this case, the model inputs for the energy system and transportation system are the same as Case 2. Instead of specifying the packet transmission profiles, the packet

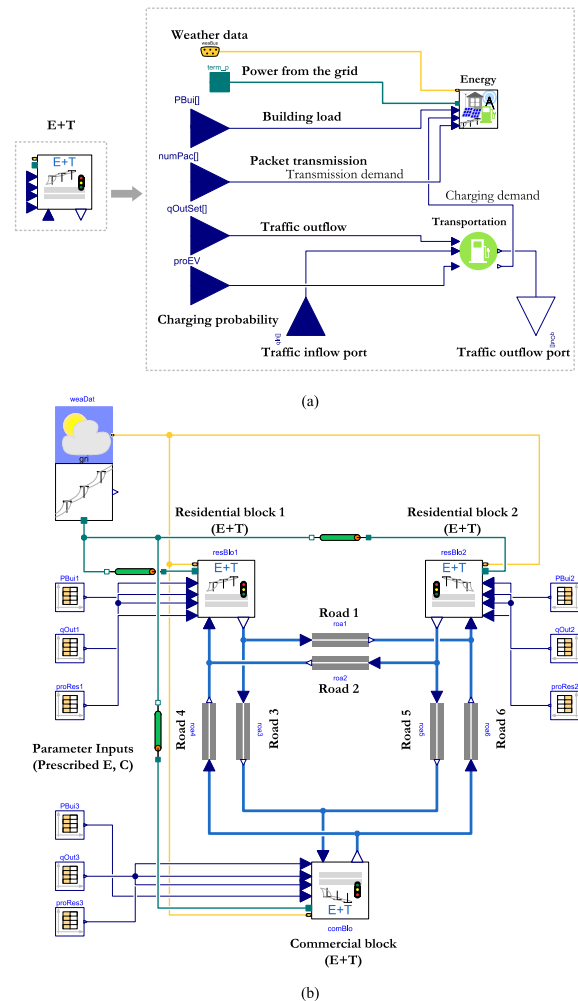


FIGURE 18. Implementation of Case 2: The (a) block icon and (b) community layer diagram for the energy and transportation (E+T) system in Modelica.

exchange processes between the road and the corresponding communication tower are modeled as described in Section III-A.2. As depicted in Fig. 20, the transmission happens between the road and the block. The assumption is made that the traffic travel time would increase due to the data loss and incomplete transmission of the traffic information.

Fig. 21 shows the interdependencies between the transportation and communication systems. Because the communication throughput far exceeds the capacity threshold during commute times, the communication packet loss (shown in Fig. 21a) surges when the average traffic flow peaks at the highest commuting times (shown in Fig. 21b). The packet loss peaks in the morning at Road 3, which is from residential block to commercial block, and in the evening at Road 6, which is from commercial block to residential block.

Comparing the simulations from all three cases produces some interesting results. Fig. 22 illustrates the impact of the communication system on the transportation system by comparing the results in Case 2 (E+T) and Case 3 (E+T+C).

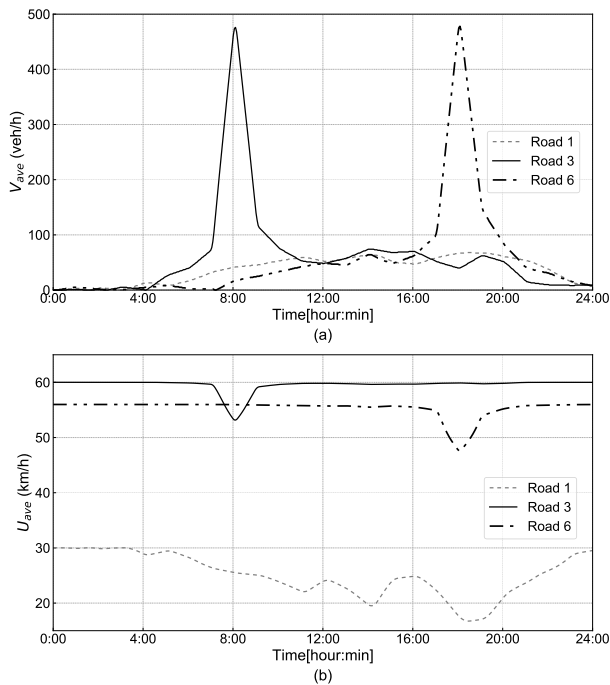


FIGURE 19. Road condition results in the connected community: (a) Average traffic flow profiles and (b) Average velocity profiles on the roads.

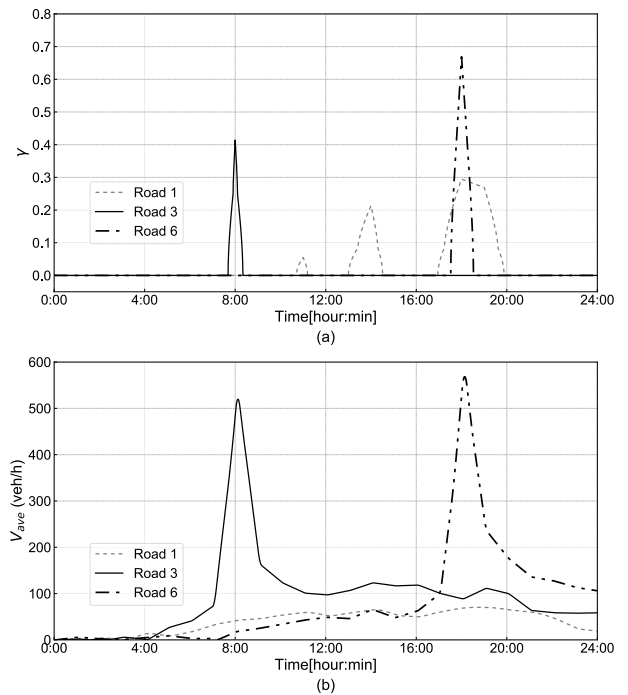


FIGURE 21. Simulated impact of transportation system on the communication system: (a) packet loss rate for the communication condition and (b) average traffic flow rate for different roads.

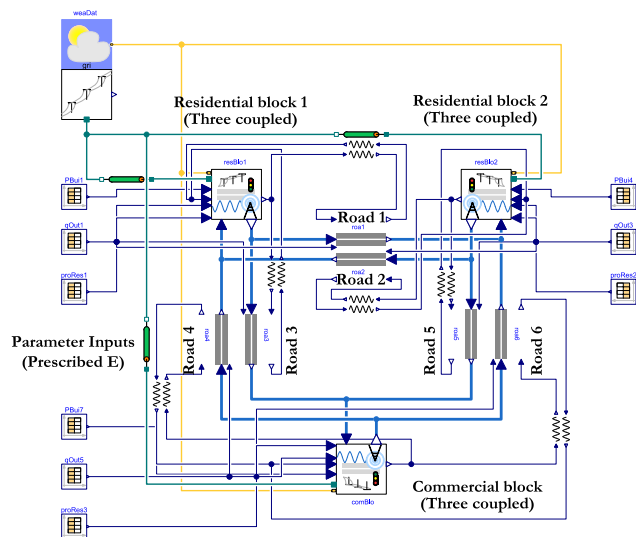


FIGURE 20. Community layer diagram for the E+T+C system in Modelica.

In low traffic hours, the results of both cases almost overlap due to the free flow condition; as such, the communication system has little impact on the traffic condition. However, at high traffic hours (around 8:00 and 18:00), the communication system deteriorates the traffic condition due to poor packet arrival rates, as shown in Case 3. Compared to Case 2, the average velocities in Case 3 are approximately 10.5% slower for the morning commute on Road 5 and 3.9% slower for the evening commute on Road 6.

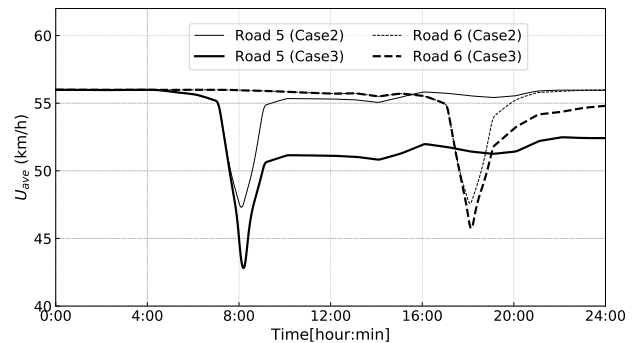


FIGURE 22. Average traffic velocities on different roads with and without modeling of the communication system.

Beyond the impact of the communication system on transportation, we can analyze the impact of the other two systems on the energy system by comparing the three considered cases. Fig. 23 shows the comparison of the calculated power draw from the grid. Clearly, we can see that there is a slight difference on the power demand from the grid during most hours; the average difference is 0.33% between Case 1 and Case 3. The deviation of power draw prediction increases during the peak commuting times (circled). This is mainly caused by the collective impacts of the transportation and communication systems. The largest deviation ratio of 7% occurs around 8:00. This will have a direct impact on the real-time unit commitment and economic dispatching of the spinning reserves, which help ensure a stable operation of the power grid. The power system would result in new

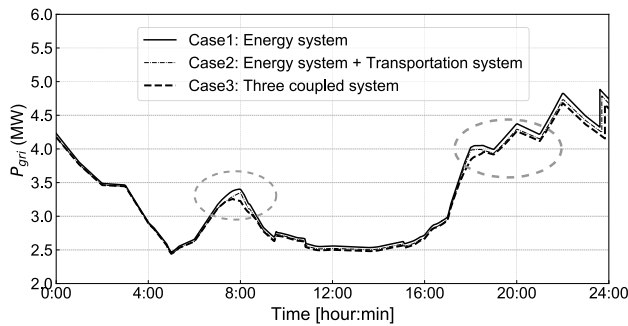


FIGURE 23. Comparison of power draw from the grid in three cases.

location marginal prices. This could in turn change the EV charging pattern and the traffic flow.

V. CONCLUSIONS

This paper proposes a new flexible and scalable multi-layer, multi-block, multi-agent (3M) approach for modeling several interconnected domains. The 3M approach is used to model the interaction of energy, transportation, and communication systems. New open source Modelica models are developed accordingly. The models are applied in three case studies to study the underlying interdependencies of the three systems for evaluating typical SCC operation. Simulation results show that the interaction among these three systems should not be neglected. In this study, the deviation of the average velocity on the road can be 10.5% with or without considering the communication system at the peak commute time. The deviation of the power draw from the grid can be 7% with or without considering the transportation and communication systems.

While these results demonstrate a successful implementation of the proposed 3M modeling framework to study interdependent infrastructure systems, further work is yet needed. The case studies included here are the first steps towards modeling of the SCC; as such, they do not fully encapsulate the interdependencies present among these three systems. Our current focus was to provide the framework which can be later extended. In the future, we plan to implement the proposed modeling framework to study applications in SCC operation, including dynamic modeling and optimization, resilience analysis, and integrated decision making.

ACKNOWLEDGMENT

This work emerged from the IBPSA Project 1, an internationally collaborative project conducted under the umbrella of the International Building Performance Simulation Association (IBPSA). Project 1 aims to develop and demonstrate a BIM/GIS and Modelica Framework for building and community energy system design and operation.

REFERENCES

[1] S. Dhakal, "GHG emissions from urbanization and opportunities for urban carbon mitigation," *Current Opinion Environ. Sustainability*, vol. 2, no. 4, pp. 277–283, 2010.

[2] Y. Sun, H. Song, A. J. Jara, and R. Bie, "Internet of Things and big data analytics for smart and connected communities," *IEEE Access*, vol. 4, pp. 766–773, 2016. doi: 10.1109/ACCESS.2016.2529723.

[3] T. Zeng, O. Semiari, W. Saad, and M. Bennis. (2018). "Joint communication and control for wireless autonomous vehicular platoon systems." [Online]. Available: <https://arxiv.org/abs/1804.05290>

[4] A. Ferdowsi, S. Ali, W. Saad, and N. B. Mandayam. (2018). "Cyber-physical security and safety of autonomous connected vehicles: Optimal control meets multi-armed bandit learning." [Online]. Available: <https://arxiv.org/abs/1812.05298>

[5] M. Mozaffari, W. Saad, M. Bennis, and M. Debbah, "Unmanned aerial vehicle with underlaid device-to-device communications: Performance and tradeoffs," *IEEE Trans. Wireless Commun.*, vol. 15, no. 6, pp. 3949–3963, Jun. 2016.

[6] Z. Dawy, W. Saad, A. Ghosh, J. G. Andrews, and E. Yaacoub, "Toward massive machine type cellular communications," *IEEE Wireless Commun.*, vol. 24, no. 1, pp. 120–128, Feb. 2017.

[7] Z. Yang, M. Chen, W. Saad, and M. Shikh-Bahaei. (2019). "Optimization of rate allocation and power control for rate splitting multiple access (RSMA)." [Online]. Available: <https://arxiv.org/abs/1903.08068>

[8] S. M. Rinaldi, J. P. Peerenboom, and T. K. Kelly, "Identifying, understanding, and analyzing critical infrastructure interdependencies," *IEEE Control Syst. Mag.*, vol. 21, no. 6, pp. 11–25, Dec. 2011.

[9] B. Robert, M. H. Senay, M.-E. P. Plamondon, and J. P. Sabourin, *Characterization and Ranking of Links Connecting Life Support Networks. Public Safety and Emergency Preparedness*. Ottawa, ON, Canada: Public Safety Canada, 2003.

[10] M. Ouyang, "Review on modeling and simulation of interdependent critical infrastructure systems," *Rel. Eng. Syst. Saf.*, vol. 121, pp. 43–60, Jan. 2014.

[11] A. Ipakchi and F. Albuyeh, "Grid of the future," *IEEE Power Energy Mag.*, vol. 7, no. 2, pp. 52–62, Mar./Apr. 2009.

[12] M. H. Amini and O. Karabasoglu, "Optimal operation of interdependent power systems and electrified transportation networks," *Energies*, vol. 11, no. 1, pp. 196–211, 2018.

[13] S. M. Rinaldi, "Modeling and simulating critical infrastructures and their interdependencies" in *Proc. 37th Hawaii Int. Conf. Syst. Sci.*, 2004, pp. 1–8.

[14] C. F. Reinhart and C. C. Davila, "Urban building energy modeling—A review of a nascent field," *Building Environ.*, vol. 97, pp. 196–202, Feb. 2016.

[15] C. C. Davila, C. F. Reinhart, and J. L. Bemis, "Modeling Boston: A workflow for the efficient generation and maintenance of urban building energy models from existing geospatial datasets," *Energy*, vol. 117, pp. 237–250, Dec. 2016.

[16] Y. Chen, T. Hong, and M. A. Piette, "Automatic generation and simulation of urban building energy models based on city datasets for city-scale building retrofit analysis," *Appl. Energy*, vol. 205, pp. 323–335, Nov. 2017.

[17] P. Remmen, M. Lauster, M. Mans, M. Fuchs, T. Osterhage, and D. Müller, "TEASER: An open tool for urban energy modelling of building stocks," *J. Building Perform. Simul.*, vol. 11, no. 1, pp. 84–98, 2018.

[18] Y. Chen, W. Li, Y. Guo, and Y. Wu, "Dynamic graph hybrid automata: A modeling method for traffic network," in *Proc. IEEE 18th Int. Conf. Intell. Transp. Syst. (ITSC)*, Sep. 2015, pp. 1396–1401.

[19] M. Jakob and Z. Moler, "Modular framework for simulation modelling of interaction-rich transport systems," in *Proc. IEEE 16th Int. Conf. Intell. Transp. Syst. (ITSC)*, Oct. 2013, pp. 2152–2159.

[20] J.-I. Latorre-Biel, J. Faulin, and E. Jiménez, and A. A. Juan, "Simulation model of traffic in smart cities for decision-making support: Case study in Tudela (Navarre, Spain)," in *Proc. Int. Conf. Smart Cities*. Cham, Switzerland: Springer, 2017, pp. 144–153.

[21] G. Suci, C. Butca, C. Dobre, and C. Popescu, "Smart city mobility simulation and monitoring platform," in *Proc. 21st Int. Conf. Control Syst. Comput. Sci. (CSCS)*, May 2017, pp. 685–689.

[22] G. A. Wainer, "Developing a software toolkit for urban traffic modeling," *Softw. Pract. Exper.*, vol. 37, no. 13, pp. 1377–1404, 2007.

[23] T. R. Henderson, M. Lacage, G. F. Riley, C. Dowell, and J. Kopena, "Network simulations with the ns-3 simulator," *SIGCOMM Demonstration*, vol. 14, no. 14, p. 527, 2008.

[24] A. Varga and R. Hornig, "An overview of the OMNeT++ simulation environment," in *Proc. 1st Int. Conf. Simulation Tools Techn. Commun., Netw. Syst. Workshops. ICST (Inst. Comput. Sci., Social-Inform. Telecommun. Eng.)*, Mar. 2008, p. 60.

- [25] Y. Cao et al., "A cost-efficient communication framework for battery-switch-based electric vehicle charging," *IEEE Commun. Mag.*, vol. 55, no. 5, pp. 162–169, May 2017.
- [26] B. Chen and H. H. Cheng, "A review of the applications of agent technology in traffic and transportation systems," *IEEE Trans. Intell. Transp. Syst.*, vol. 11, no. 2, pp. 485–497, Jun. 2010.
- [27] P. Palensky, A. A. V. D. Meer, C. D. Lopez, A. Joseph, and K. Pan, "Cosimulation of intelligent power systems: Fundamentals, software architecture, numerics, and coupling," *IEEE Ind. Electron. Mag.*, vol. 11, no. 1, pp. 34–50, Mar. 2017.
- [28] A. Ferdowsi, A. Sanjab, W. Saad, and N. B. Mandayam, "Game theory for secure critical interdependent gas-power-water infrastructure," in *Proc. Resilience Week (RWS)*, Sep. 2017, pp. 184–190.
- [29] A. Ferdowsi, W. Saad, and N. B. Mandayam. (2017). "Colonel blotto game for secure state estimation in interdependent critical infrastructure." [Online]. Available: <https://arxiv.org/abs/1709.09768>
- [30] G. Satumtira and L. Dueñas-Osorio, "Synthesis of modeling and simulation methods on critical infrastructure interdependencies research," in *Sustainable and Resilient Critical Infrastructure Systems*. Berlin, Germany: Springer, 2010, pp. 1–51.
- [31] S. V. Buldyrev, R. Parshani, G. Paul, H. E. Stanley, and S. Havlin, "Catastrophic cascade of failures in interdependent networks," *Nature*, vol. 464, no. 7291, p. 1025, 2010.
- [32] V. Rosato, L. Issacharoff, F. Tiriticco, S. Meloni, S. Porcellinis, and R. Setola, "Modelling interdependent infrastructures using interacting dynamical models," *Int. J. Crit. Infrastruct.*, vol. 4, nos. 1–2, pp. 63–79, 2008.
- [33] D. T. Nguyen, Y. Shen, and M. T. Thai, "Detecting critical nodes in interdependent power networks for vulnerability assessment," *IEEE Trans. Smart Grid*, vol. 4, no. 1, pp. 151–159, Mar. 2013.
- [34] A. Bernstein, D. Bienstock, D. Hay, M. Uzunoglu, and G. Zussman, "Power grid vulnerability to geographically correlated failures—Analysis and control implications," in *Proc. IEEE INFOCOM Conf. Comput. Commun.*, Apr./May 2014, pp. 2634–2642.
- [35] C. Heracleous, P. Kolios, C. G. Panayiotou, G. Ellinas, and M. M. Polycarpou, "Hybrid systems modeling for critical infrastructures interdependency analysis," *Rel. Eng. Syst. Saf.*, vol. 165, pp. 89–101, Sep. 2017.
- [36] Z. Cao, S. Jiang, J. Zhang, and H. Guo, "A unified framework for vehicle rerouting and traffic light control to reduce traffic congestion," *IEEE Trans. Intell. Transp. Syst.*, vol. 18, no. 7, pp. 1958–1973, Jul. 2017.
- [37] A. M. Farid, "A hybrid dynamic system model for multimodal transportation electrification," *IEEE Trans. Control Syst. Technol.*, vol. 25, no. 3, pp. 940–951, May 2017.
- [38] W. Su, J. Wang, K. Zhang, and M.-Y. Chow, "Framework for investigating the impact of PHEV charging on power distribution system and transportation network," in *Proc. IEEE 38th Annu. Conf. Ind. Electron. Soc.*, Oct. 2012, pp. 4735–4740.
- [39] K. Hopkinson, X. Wang, R. Giovanini, J. Thorp, K. Birman, and D. Coury, "EPOCHS: A platform for agent-based electric power and communication simulation built from commercial off-the-shelf components," *IEEE Trans. Power Syst.*, vol. 21, no. 2, pp. 548–558, May 2006.
- [40] H. Georg and S. C. Müller, C. Rehtanz, and C. Wietfeld, "Analyzing cyber-physical energy systems: The INSPIRE cosimulation of power and ICT systems using HLA," *IEEE Trans. Ind. Inform.*, vol. 10, no. 4, pp. 2364–2373, Nov. 2014.
- [41] S. Chatzivasileiadis et al., "Cyber-physical modeling of distributed resources for distribution system operations," *Proc. IEEE*, vol. 104, no. 4, pp. 789–806, Apr. 2016.
- [42] C. Sommer, R. German, and F. Dressler, "Bidirectionally coupled network and road traffic simulation for improved IVC analysis," *IEEE Trans. Mobile Comput.*, vol. 10, no. 1, pp. 3–15, Jan. 2011.
- [43] R. Fernandes, F. Vieira, and M. Ferreira, "VNS: An integrated framework for vehicular networks simulation," in *Proc. IEEE Veh. Netw. Conf. (VNC)*, Nov. 2012, pp. 195–202.
- [44] S. Zemouri, S. Mehar, and S.-M. Senouci, "HINTS: A novel approach for realistic simulations of vehicular communications," in *Proc. Global Inf. Infrastruct. Netw. Symp. (GIIS)*, Dec. 2012, pp. 1–6.
- [45] B. Schünemann, "V2X simulation runtime infrastructure VSimRTI: An assessment tool to design smart traffic management systems," *Comput. Netw.*, vol. 55, no. 14, pp. 3189–3198, Oct. 2011.
- [46] L. Bedogni, L. Bononi, A. Borghetti, R. Bottura, and A. D'Elia, and T. S. Cinotti, "Integration of traffic and grid simulator for the analysis of e-mobility impact on power distribution networks," in *Proc. IEEE Eindhoven PowerTech*, Jun./Jul. 2015, pp. 1–6.
- [47] P. Palensky, A. van der Meer, C. Lopez, A. Joseph, and K. Pan, "Applied cosimulation of intelligent power systems: Implementing hybrid simulators for complex power systems," *IEEE Ind. Electron. Mag.*, vol. 11, no. 2, pp. 6–21, Jun. 2017.
- [48] M. Tiller, *Introduction to Physical Modeling with Modelica*. New York, NY, USA: Springer, 2001.
- [49] S. Huang, W. Zuo, and M. D. Sohn, "Improved cooling tower control of legacy chiller plants by optimizing the condenser water set point," *Building Environ.*, vol. 111, pp. 33–46, Jan. 2017.
- [50] W. Tian, T. A. Sevilla, W. Zuo, and M. D. Sohn, "Coupling fast fluid dynamics and multizone airflow models in Modelica Buildings library to simulate the dynamics of HVAC systems," *Building Environ.*, vol. 122, pp. 269–286, Sep. 2017.
- [51] R. Al Junaibi and A. M. Farid, "A method for the technical feasibility assessment of electrical vehicle penetration," in *Proc. IEEE Int. Syst. Conf. (SysCon)*, Apr. 2013, pp. 606–611.
- [52] M. Stifter and S. Übermasser, "Dynamic simulation of power system interaction with large electric vehicle fleet activities," in *Proc. IEEE Grenoble Conf.*, Jun. 2013, pp. 1–6.
- [53] F. Montori, A. Borghetti, and F. Napolitano, "A co-simulation platform for the analysis of the impact of electromobility scenarios on the urban distribution network," in *Proc. IEEE 2nd Int. Forum Res. Technol. Soc. Ind. Leveraging Better Tomorrow (RTSI)*, Sep. 2016, pp. 1–6.
- [54] K. Anderson, J. Du, A. Narayan, and A. El Gamal, "Gridspice: A distributed simulation platform for the smart grid," *IEEE Trans. Ind. Inform.*, vol. 10, no. 4, pp. 2354–2363, Nov. 2014.
- [55] C. Shum et al., "HLA based co-simulation framework for multiagent-based smart grid applications," in *Proc. IEEE PES Asia-Pacific Power Energy Eng. Conf. (APPEEC)*, Dec. 2014, pp. 1–6.
- [56] A. N. Albagli, D. M. Falcão, and J. F. de Rezende, "Smart grid framework co-simulation using HLA architecture," *Electr. Power Syst. Res.*, vol. 130, pp. 22–33, Jan. 2016.
- [57] M. Rondinone et al., "iTETRIS: A modular simulation platform for the large scale evaluation of cooperative ITS applications," *Simul. Model. Pract. Theory*, vol. 34, pp. 99–125, May 2013.
- [58] Z. Cao, H. Guo, J. Zhang, and U. Fastenrath, "Multiagent-based route guidance for increasing the chance of arrival on time," in *Proc. 30th AAAI Conf. Artif. Intell.*, Mar. 2016, pp. 3814–3820.
- [59] Z. Cao, H. Guo, and J. Zhang, "A multiagent-based approach for vehicle routing by considering both arriving on time and total travel time," *ACM Trans. Intell. Syst. Technol. (TIST)*, vol. 9, no. 3, p. 25, 2018.
- [60] S. Civanlar, J. J. Grainger, H. Yin, and S. S. H. Lee, "Distribution feeder reconfiguration for loss reduction," *IEEE Trans. Power Del.*, vol. PWRD-3, no. 3, pp. 1217–1223, Jul. 1988.
- [61] M. Wetter, "Multizone building model for thermal building simulation in modelica," in *Proc. Modelica Conf.*, Sep. 2006, pp. 517–526.
- [62] X. Li and J. Wen, "Building energy consumption on-line forecasting using physics based system identification," *Energy Buildings*, vol. 82, pp. 1–12, Oct. 2014.
- [63] K. Qian, C. Zhou, M. Allan, and Y. Yuan, "Modeling of load demand due to EV battery charging in distribution systems," *IEEE Trans. Power Syst.*, vol. 26, no. 2, pp. 802–810, May 2011.
- [64] G. Chen, C. Li, M. Ye, and J. Wu, "An unequal cluster-based routing protocol in wireless sensor networks," *Wireless Netw.*, vol. 15, no. 2, pp. 193–207, 2009.
- [65] M. Wetter, M. Bonvini, T. S. Noudui, and W. Zuo, "Modelica buildings library 2.0," in *Proc. 14th Int. Conf. Int. Building Perform. Simulation Assoc. (Building Simulation)*, Dec. 2015, pp. 387–394.
- [66] B. Seibold, *A Mathematical Introduction to Traffic Flow Theory*. Los Angeles, CA, USA: Institute for Pure and Applied Mathematics, 2015.
- [67] S. P. Hoogendoorn and P. H. L. Bovy, "State-of-the-art of vehicular traffic flow modelling," *Proc. Inst. Mech. Eng., I, J. Syst. Control Eng.*, vol. 215, no. 4, pp. 283–303, 2001.
- [68] W. Wei, "Practical speed-flow relationship model of highway traffic-flow," *J. Southeast Univ. (Natural Sci. Ed.)*, vol. 33, no. 4, pp. 487–491, 2003.
- [69] M. Peng, N. Xiong, G. Xie, and L. T. Yang, "The weighted shortest path search in mobile GIS services," in *Advances in Grid and Pervasive Computing*, 2008, pp. 384–395.

- [70] E. Sortomme, M. M. Hindi, S. D. J. MacPherson, and S. S. Venkata, "Coordinated charging of plug-in hybrid electric vehicles to minimize distribution system losses," *IEEE Trans. Smart Grid*, vol. 2, no. 1, pp. 198–205, Mar. 2011.
- [71] Z. Liu, W. Hou, Y. Li, and Q. Chen, "Research of packet loss model in wireless Ad hoc networks," *Comput. Eng. Appl.*, vol. 45, no. 9, pp. 108–109, 2009.
- [72] K. C. Ang and K. S. Neo, "Real-life application of a simple continuum traffic flow model," *Int. J. Math. Edu. Sci. Technol.*, vol. 36, no. 8, pp. 913–922, 2005.
- [73] E. J. Palacios-Garcia, A. Moreno-Munoz, I. Santiago, I. M. Moreno-Garcia, and R. J. Real-Calvo, "Study of a smart energy community PV and storage requirements: A modeling approach towards net-zero energy," in *Proc. ENERGY 6th Int. Conf. Smart Grids, Green Commun. IT Energy-Aware Technol.*, 2016, pp. 37–41.
- [74] M. Deru et al., *U.S. Department of Energy Commercial Reference Building Models of the National Building Stock*. Golden, Colorado: National Renewable Energy Laboratory, 2011.
- [75] U.S. Department of Energy. *Commercial and Residential Hourly Load Profiles for all TMY3 Locations in the United States*. Accessed: Dec. 3, 2017. [Online]. Available: <https://openei.org/datasets/files/961/pub/>
- [76] O.W. A. Martin and N. A. McGuckin, "Travel Estimation Techniques for Urban Planning," Nat. Academies Press, Washington, DC, USA, Tech. Rep. 365, 1998.



cyber-physical systems.

XING LU received the B.S. degree and M.Eng. degree in power engineering from Tongji University, Shanghai, China, in 2014 and 2016, respectively. He is currently pursuing the Ph.D. degree with the University of Colorado, Boulder, CO, USA. He has been with the Sustainable Building Systems Laboratory (SBS Lab), CU Boulder, since 2017, with Dr. W. Zuo as his Advisor. His research interests include the modeling and simulation of building systems, urban energy systems, and large



Sustainable Technologies Laboratory, University of California at Berkeley. Since 2018, she has been a Teaching Assistant with the Department of Civil, Environmental and Architectural Engineering, University of Colorado Boulder. Her research interests include modeling of smart and connected communities, healthy buildings, district energy systems, and sustainable energy systems for low-income populations. She is a Student Member of ASHRAE, ICC, and IBPSA.

KATHRYN HINKELMAN received the B.S. degree in mechanical engineering from the University of Denver, Denver, CO, USA, in 2013, and the M.S. degree in mechanical engineering from the University of California at Berkeley, Berkeley, CA, USA, in 2015. She is currently pursuing the Ph.D. degree in architectural engineering with the University of Colorado Boulder, Boulder, CO, USA. From 2014 to 2015, she was a Graduate Student Researcher with the Berkeley Energy and



Engineer with Tongji University, Shanghai, China. Since 2017, he has been a Research Assistant with the Department of Civil, Environmental and Architectural Engineering, University of Colorado Boulder. His research interests include equation-based modeling, simulation and optimization, data center demand response, and grid-interactive buildings.

YANGYANG FU (S'19) received the B.S. degree in civil engineering from the PLA University of Science and Technology, Nanjing, China, in 2012, and the M.S. degree in mechanical engineering from Tongji University, Shanghai, China, in 2016. He is currently pursuing the Ph.D. degree in architectural engineering with the University of Colorado Boulder, Boulder, CO, USA. From 2013 to 2016, he was a Research Assistant with the Institute of Heating and a Ventilation and Air Conditioning



worked on building reduced-order model development for control deployment and aggregated building load flexibility quantification. Her current research interests include resilient energy systems, building energy system modeling and control, and building-to-grid integration. She is also an ASHRAE Student Member.

JING WANG received the B.Eng. degree in built environment and equipment engineering from Tongji University, Shanghai, China, in 2013, and the M.S. degree in mechanical engineering from the Technical University of Braunschweig, Braunschweig, Germany, in 2017. She is currently pursuing the Ph.D. degree in architectural engineering with the University of Colorado Boulder, Boulder, CO, USA. In 2018, she took an internship at the Pacific Northwest National Laboratory, where she



He was an Assistant Professor with the University of Miami and a Computational Research Scientist with the Lawrence Berkeley National Laboratory. He is currently an Associate Professor and a Lewis-Worcester Faculty Fellow with the Department of Civil, Environmental and Architectural Engineering, University of Colorado Boulder, Boulder, CO, USA. He also has a joint appointment with the National Renewable Energy Laboratory, Commercial Buildings Group, Golden, CO, USA. He was a recipient of the ASCE ExCEED Fellowship, the IBPSA-USA Emerging Professional Award, the Eliahu I. Jury Early Career Research Award, the ASHRAE Distinguished Service Award, the Provost Research Award, and the SEEDS Leadership Award. He also served as the Founding Chair of the IBPSA-USA Research Committee and a Voting Member of the ASHRAE TC 4.7 Energy Calculations. He currently serves as a Treasurer and the Affiliate Director (representing USA) of the International Building Performance Simulation Association (IBPSA), the Chair and a Voting Member of the ASHRAE Technical Committee (TC) 7.4 Exergy Analysis for Sustainable Buildings, and the Vice Chair of ASHRAE (TC) 4.10 Indoor Environment Modeling.

WANGDA ZUO received the B.S. degree and M.Eng. degree in automation from Chongqing University, Chongqing, China, in 2000 and 2003, respectively, the M.Sc. degree in computational engineering from Friedrich-Alexander-University Erlangen-Nuremberg, Erlangen, Germany, in 2005, and the Ph.D. degree in mechanical engineering from Purdue University, West Lafayette, IN, USA, in 2010.



QIANQIAN ZHANG (S'16) received the B.S. degree in telecommunication engineering with management from the Beijing University of Posts and Telecommunications, Beijing, China, in 2015. She is currently pursuing the Ph.D. degree with the Bradley Department of Electrical and Computer Engineering, Virginia Tech, Blacksburg, VA, USA. Her research interests include wireless communication, unmanned aerial vehicle (UAV) communications, and machine learning.



WALID SAAD (S'07–M'10–SM'15–F'19) received the Ph.D. degree from the University of Oslo, in 2010.

He is currently an Associate Professor with the Department of Electrical and Computer Engineering, Virginia Tech, where he leads the Network Science, Wireless, and Security laboratory. His research interests include wireless networks, machine learning, game theory, security, unmanned aerial vehicles, cyber-physical systems, and network science. He was a recipient of the NSF CAREER Award, in 2013, the AFOSR Summer Faculty Fellowship, in 2014, and the Young Investigator Award from the Office of Naval Research (ONR), in 2015. He was the author/coauthor of seven conference best paper awards at WiOpt, in 2009, ICIMP, in 2010, IEEE WCNC, in 2012, IEEE PIMRC, in 2015, the IEEE SmartGridComm, in 2015, EuCNC, in 2017, and the IEEE GLOBECOM, in 2018. He was also a recipient of the 2015 Fred W. Ellersick Prize from the IEEE Communications Society, the 2017 IEEE ComSoc Best Young Professional in Academia Award, and the 2018 IEEE ComSoc Radio Communications Committee Early Achievement Award. From 2015 to 2017, he was named the Stephen O. Lane Junior Faculty Fellow at Virginia Tech. In 2017, he was named the College of Engineering Faculty Fellow. He also serves as an Editor for the IEEE TRANSACTIONS ON WIRELESS COMMUNICATIONS, IEEE TRANSACTIONS ON MOBILE COMPUTING, IEEE TRANSACTIONS ON COGNITIVE COMMUNICATIONS AND NETWORKING, and IEEE TRANSACTIONS ON INFORMATION FORENSICS AND SECURITY. He is also the Editor-at-Large of the IEEE TRANSACTIONS ON COMMUNICATIONS. He is also an IEEE Distinguished Lecturer.

• • •